# Charge carrier mobility in disordered organic blends for photovoltaics

L. J. A. Koster
*Molecular Materials and Nanosystems, Eindhoven University of Technology, P.O. Box 513, 5600 MB Eindhoven, The Netherlands*
(Received 9 February 2010; revised manuscript received 29 April 2010; published 24 May 2010)

Charge transport in disordered organic blends is studied theoretically by numerically solving the Pauli master equation. The influence of morphology, disorder, electric field, and charge carrier concentration on blend mobility is assessed. Important differences between neat materials and blends are found. The dependence of mobility on charge carrier concentration is more pronounced in blends and it is influenced by the electric field strength. At low charge carrier densities, blend mobility is found to decrease with increasing field. Additionally, the impact of the volume ratio of the constituent materials and their domain size on the mobility is presented. Especially for strongly disordered materials charge transport is favored by relatively large domains. To compare these theoretical findings with existing experimental mobility data, the current density in a space-charge-limited device is computed. The author finds that, for the parameters and morphologies studied, the apparent mobility in such a device decreases with increasing bias voltage.

DOI: 10.1103/PhysRevB.81.205318 PACS number(s): 73.61.Ph, 72.80.Le, 72.20.Ee

## I. INTRODUCTION

Organic semiconductors hold great promise for a variety of optoelectronic devices: light-emitting diodes,[1] field-effect transistors,[2] and photovoltaic cells.[3,4] Blending of organic materials is an attractive approach to optimize and tune the properties of the materials for device applications.[5–10] Additionally, blending can result in new phenomena and properties as a result of intermolecular interactions, self-organization (or its frustration), and confinement effects.[7,11]

In organic photovoltaic devices it is especially critical to use a blend rather than a neat material. Due to the low dielectric constant typical for organic materials the probability of forming free charges upon light absorption is very low. Instead, strongly bound excitons are formed with a binding energy of around 0.4 eV in the case of the prototypical polymer poly(phenylene vinylene).[12–14] The large interface between the components acts to dissociate excitons that have been photogenerated in either material, thereby generating separate charges that can travel to different electrodes and yield a photocurrent. In polymer light-emitting devices, the two components are responsible for transporting electrically injected charges toward the interface, where radiative recombination may occur. Charge transport and its dependence on blend morphology is fundamental to all these devices.

Unsurprisingly, charge transport in photovoltaic blends has been studied theoretically. Frost *et al.*[15] studied the effect of morphology on charge transport and photocurrent generation in polymer blends used for photovoltaics by a Monte Carlo approach. By varying the interaction energies between the polymer chains, polymer films following different process treatments were represented. They found that morphology strongly influences charge-transport characteristics, such as the percolation threshold, mobility, and dispersion.

In a dynamic Monte Carlo simulation of polymer blend photovoltaic devices, the impact of feature size on charge-transport efficiency and overall solar-cell performance has been studied by Meng *et al.*[16] They found that the optimal energy conversion efficiency is reached when the feature size is around 10 nm. This comprehensive model is geared toward describing overall performance rather than studying charge carrier mobility.

It is well known from experiments that the local morphology may not be uniform throughout the film.[17–22] Groves *et al.*[23] have studied the impact of composition, domain size, and energetic disorder on the mobility of carriers in an organic donor-acceptor blend and assessed the influence of nonhomogeneity. These simulations show that, for the changes in local morphology expected within the thickness of a typical bulk heterojunction photovoltaic device, changes in mobility of more than an order of magnitude are expected, leading to potential loss in device performance.

Notwithstanding the importance of these studies, they do not explicitly describe the field- and carrier-density dependence of blend mobility as they are either conducted in the low-density limit at constant-field strength,[23] at fixed finite density and varying-field strength,[15] or focus on transport efficiency rather than mobility.[16] Consequently, an explicit description of the field- and carrier-density dependence of the mobility in blends is still lacking. As mobility measurements are performed at varying, finite density and field strength, it is important to consider both parameters in an attempt to describe experimental mobility data.

In this paper, we study charge transport in disordered organic blends as a function of carrier density and field strength. By numerically solving the Pauli master equation,[24] the mobility of carriers in one phase of a binary blend is calculated for various feature sizes and blend composition ratios. Compared with Monte Carlo simulations the master equation approach has several advantages. It is convenient for considering density-dependent effects and is numerically more efficient. This approach was used to study field and density dependences of the mobility in neat conjugated polymers,[24,25] carrier injection into such films,[26] as well as devices thereof.[27] Zhou *et al.*[28] showed that master equation mobility results coincide with Monte Carlo simulations that account for the carrier-carrier Coulomb interactions up to densities of around $10^{-2}$. This paper is organized as follows. First, field and density dependences of the mobility in neat and blended organic materials are compared. Next, the influence of blend stoichiometry on blend mobility is addressed.

 

In order to estimate the combined effect of density and field on mobility the current density in a space-charge-limited (SCL) diode is calculated by using a drift-diffusion approach.

## II. MODEL

We represent the morphology as a three-dimensional (3D) regular 1 nm Cartesian lattice comprising transporting and nontransporting sites extending typically $L=150$ sites in every direction. Initially, sites are randomly chosen to be either transporting or nontransporting (according to the desired volume ratio $\alpha$ of transporting sites to the total volume). Subsequent coarsening of this morphology is achieved by simulated annealing.[5,29] Briefly, this technique involves randomly choosing a pair of neighboring sites and probabilistically admitting a swap based on the energy of the system. As cyclic boundary conditions are used for transport, pairwise swaps over matching faces of the morphology are also allowed. Phase separation is encouraged by choosing the interfacial energies of the constituent phases such that a configuration with a smaller interfacial area is lower in energy. The average domain size $b$ of the minority component is determined from

$$b = \frac{6\ \min(\alpha, 1-\alpha)V}{A}, \tag{1}$$

where $V$ is the total volume and $A$ is the interfacial area. Next, each transport site is assigned a site-energy $\epsilon_i$ according to Gaussian distribution of standard deviation $\sigma$. This Gaussian density of states reflects the energetic spread in the transport sites due to disorder. For organic materials $\sigma$ is typically around 0.1 eV;[30–34] this value is used throughout this paper unless stated otherwise. To sample the average behaviors of carriers, multiple morphologies with the same characteristics ($b$, $\alpha$, and $\sigma$) are generated.

Charge carriers hop from site $i$ to site $j$ with a rate given by the Miller-Abrahams expression

$$W_{i\to j} = \begin{cases} \nu \exp(-\Delta E_{ij}/k_B T) & \text{if } \Delta E_{ij} > 0, \\ \nu & \text{otherwise}, \end{cases} \tag{2}$$

where $\nu$ is the attempt-to-jump frequency which we take $\nu = 10^{12}$ s$^{-1}$. This value is chosen such that the low-field mobility in neat material is approximately $10^{-8}$ m$^2$/V s in the low-carrier-density limit. However, it should be noted that the hopping rates $W_{i\to j}$, and hence the mobility, are linearly proportional to $\nu$, so that this choice of $\nu$ does not result in a loss of generality. The energy difference between sites $i$ and $j$ is given by

$$\Delta E_{ij} = \epsilon_j - \epsilon_i - q\vec{F}\cdot(\vec{r}_j - \vec{r}_i). \tag{3}$$

We study the motion of charge carriers in a 3D lattice by solving the steady-state Pauli master equation

$$\Sigma_j [W_{i\to j} n_i (1-n_j) - W_{j\to i} n_j (1-n_i)] = 0 \tag{4}$$

with the rates $W_{i\to j}$ given by Eq. (2). In Eq. (4) double occupation of a site has been excluded. Carrier hops are restricted to occur between nearest-neighbor sites only, which is valid in the $\sigma/k_B T$ range used in the present work.[35] Following Yu *et al.*[24] we solve the Pauli master equation by calculating $n_i$ from

$$n_i = \frac{\Sigma_j W_{j\to i} n_j}{\Sigma_j [W_{i\to j}(1-n_j) + W_{j\to i} n_j]} \tag{5}$$

while ensuring that the overall carrier density is conserved. This procedure is repeated until convergence is reached.

Once the Pauli master equation has been solved for $n_i$, the mobility $\mu$ is calculated from

$$\mu = \frac{\Sigma_{ij} W_{i\to j} n_i (1-n_j)(\vec{r}_j - \vec{r}_i)\cdot \hat{F}}{N_0 L^3 |\vec{F}|}, \tag{6}$$

where $\vec{F}$ denotes the electric field, $\hat{F}=\vec{F}/|\vec{F}|$, and $N_0$ is the average carrier density.

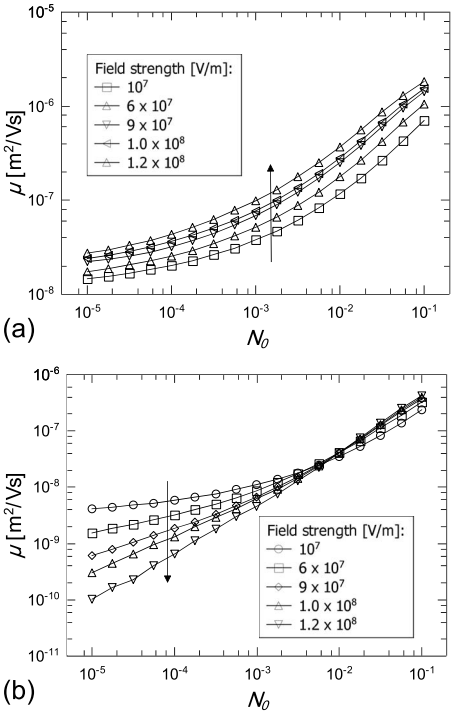


FIG. 1. Density dependence of the mobility in (a) a neat material and (b) a blend ($\alpha$=0.5, $b$=6 nm).

## III. RESULTS AND DISCUSSION

### A. Carrier density and field dependence

Figure 1(a) shows the calculated mobility of a neat material as a function of density $N_0$. In accordance with previous reports,[25,36–38] the charge carrier mobility in these neat films is found to depend both on electric field strength and charge carrier density. The enhancement of mobility at high fields is due to field-induced lowering of hopping barriers, making it easier for carriers to escape from a deep-lying energy site. The effect of carrier density is due to a gradual filling of the sites lowest in energy as the overall density increases. Once occupied, these deep-lying sites cannot accommodate other

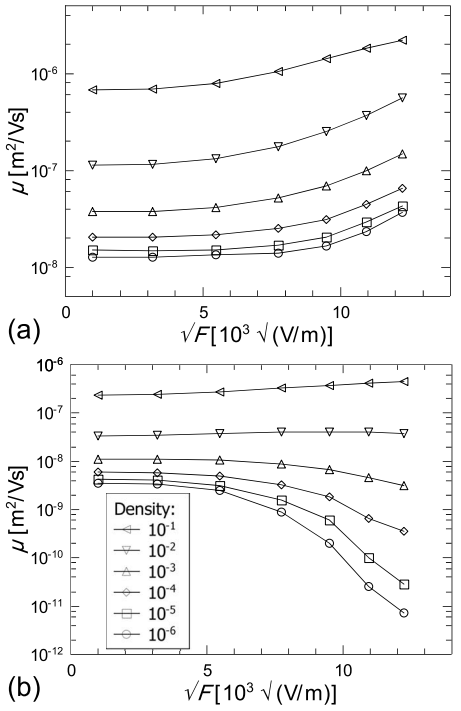


FIG. 2. Field dependence of the mobility in (a) a neat material and (b) a blend ($\alpha$=0.5, $b$=6 nm).

carriers, making it easier for the remaining carriers to move around. Hence the overall mobility increases as the charge carrier density increases. Pasveer *et al.*[25] have shown that field and density dependences of the mobility in neat polymers can be approximated by

$$\mu(T,N_0,F) \approx \mu(T,N_0)f(T,F), \tag{7}$$

where $f(T,F)$ is a density-independent function of field and temperature $T$. From Eq. (6) it is clear that this factorization is exact in the absence of disorder.

Figure 1(b) shows the mobility in a blend with volume fraction $\alpha$=0.5 and average feature size $b$=6 nm. Clearly, the behavior is quite different in the case of a blend. At low fields the mobility shows a density dependence similar to the neat case, but at higher electric fields ($>10^7$ V/m) the density dependence is much more pronounced. This implies that factorization of field and density dependences is no longer possible. Figure 2, which shows the field dependence, reinforces this point, while the factorization holds for the neat material [Fig. 2(a)], it clearly fails for the blend material [Fig. 2(b)].

The electric field dependence of the blend material is very different from that of the neat material. Whereas the mobility of the neat material increases with increasing field, the behavior of the blend material is opposite: for the blend, increasing the electric field reduces mobility. This effect was also observed by Frost *et al.*[15] Simulations with $\sigma$ ranging from 0.025 to 0.125 eV yield a similar difference between neat and blend materials, showing that this effects is not due to energetic disorder.

The behavior at low electric fields can be explained by the absence of directionality other than the electric field. This

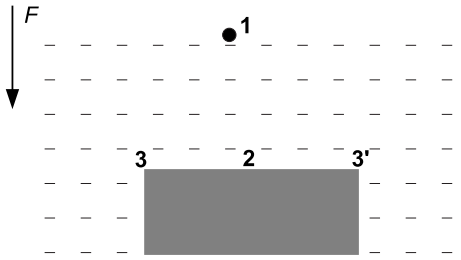


FIG. 3. Charge carrier (circle) hopping from site to site (dashes) along the field from the top 1 will encounter an obstacle (gray rectangle) at 2. The subsequent motion to 3( ′) is a diffusive process and is not directly dependent on the field strength.

implies that mobility must be an even function of electric field. Assuming it is analytical at zero field, its first derivative must be zero at zero field. This effect can be clearly seen in Figs. 2(a) and 2(b).

How can the negative field dependence and the failure of factorization be understood? Figure 3 illustrates the flow of carriers around part of the nontransporting phase. As carriers move with the field from 1 they will encounter an obstacle at 2. A carrier at 2 has three possible courses of action: it can go back to 1 or it can travel in the direction of 3 or 3′. As the field is increased, the movement back to 1 is suppressed, leaving directions 3 and 3′ as the only viable options. Hopping in this direction does not (directly) depend on the electric field strength and, thus, proceeds via diffusion. For the mobility to be constant, the current flow needs to be linearly proportional to the electric field strength. Even though the overall current can still increase with increasing field, it is no longer proportional to the field and hence the mobility decreases.

As for the effect of carrier density, if another carrier is present at the obstacle near 2, the motion of the carriers is restricted by site exclusion, making the diffusion in the directions 3 and 3′ (toward regions with lower carrier density) stronger. This implies that field and density dependences are no longer mutually independent. At high carrier densities, there would be a large number of carriers piled up at the obstacle, making it easier for new carriers (starting near 1) to avoid this region of the layer altogether. This explains why the field dependence is just positive at the highest densities (see Figs. 1 and 2), at least at the values of $\sigma$ used here.

The movement of carriers in a large volume depends on whether carriers can avoid large obstacles which can involve hops against the field. When the electric field is increased paths that force carriers to move against the field will become less operative reducing the blend mobility. This is illustrated in Fig. 4 which shows the local current flow in a blend structure. Although the overall current is higher at high fields, most of the current flows through a much smaller fraction of the volume. Therefore, the mobility in blends is lower than the neat mobility and the effect of blend morphology is reminiscent of off-diagonal disorder effects in neat materials.[39,40] If positional disorder is strong, the mobility of neat materials can also be negative.[39] Note that in the foregoing discussion no reference has been made to energetic disorder. Energetic disorder will accentuate the effects just

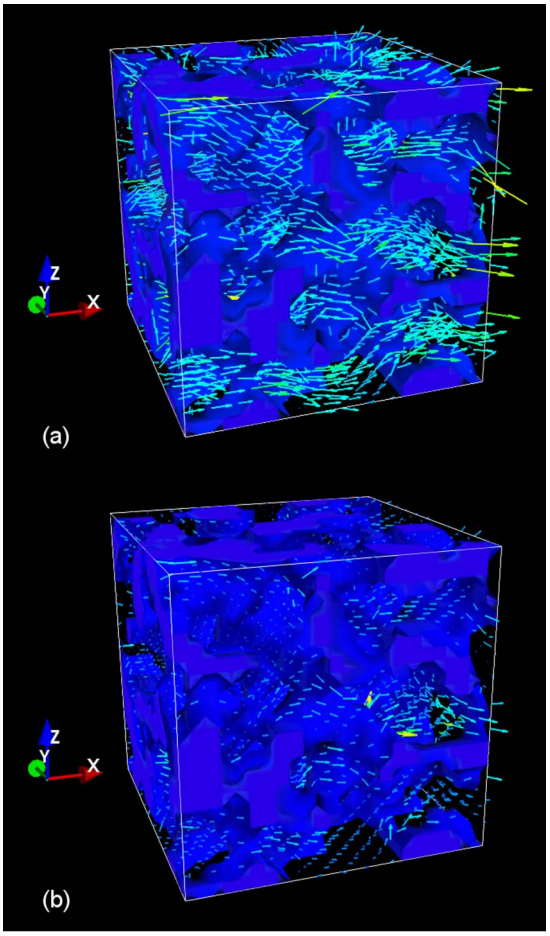


FIG. 4. (Color online) Local current (arrows, length proportional to current) in a blend with $\alpha=0.5$ and $b=5$ nm in the absence of disorder at (a) $F=10^6$ V/m and (b) $F=10^8$ V/m. The current at high-field strengths is much less homogeneous. The transporting phase appears transparent while the nontransporting phase is depicted fully opaque. The field is directed in along the $x$ axis. Note that the vectors in (a) and (b) are not drawn to the same scale.

described as paths which are energetically favored neither necessarily efficiently negotiate the blend morphology nor do they avoid dead-ends or cul-de-sacs. This is due to the presumed absence of a correlation between the energetic landscape and the real-space blend morphology.

### B. Influence of blend stoichiometry

So far, we have discussed the mobility in blends with equal volumes of both constituent phases. Figure 5 portrays the effect of volume fraction $\alpha$ on blend mobility. Clearly, as the volume fraction approaches the percolation limit, the mobility diminishes. This figure also makes clear the influence of average feature size $b$ [defined by Eq. (1)] and energetic disorder $\sigma$ on mobility. Generally, small domains and high disorder yield low mobilities.

The average feature size $b$ as defined by Eq. (1) corresponds to the average feature size of the minority component. So, for $\alpha>0.5$ the carriers move around obstacles of average size $b$, while for $\alpha<0.5$ the carriers move through a

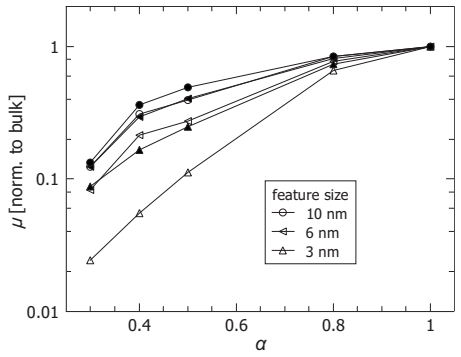


FIG. 5. Dependence of blend mobility on volume fraction at different average feature sizes $b$ of the minority component (closed $\sigma=50$ meV, open $\sigma=100$ meV). Field strength $10^6$ V/m, $N_0=10^{-5}$.

phase of average size $b$. When $\alpha<0.5$ the mobility is improved if the domain size is increased, as would be expected.[15] On the other hand, when $\alpha>0.5$ a smaller domain size implies that the nontransporting phase is better dispersed in the transporting phase. These small nontransporting features appear to be detrimental for charge transport, especially in blends with strong energetic disorder. The energetic landscape, defined by the site energies $\epsilon_i$, favors certain pathways at the expense of others, creating filaments.[41] In a blend, these filaments do not necessarily match up with the real-space blend morphology, especially when the nontransporting phase is finely dispersed in the transporting one. These findings are in accord with the results obtained by Groves *et al.*[23] who used a Monte Carlo simulation to calculate blend mobility at a field strength of $10^7$ V/m.

### C. Comparison with experimental data

McNeill and Greenham[42] measured the hole mobility in annealed blends (1:1 by weight) of poly(3-hexylthiophene) (P3HT) and poly((9,9-dioctylfluorene)-2,7-diyl-alt-[4,7-bis(3-hexylthien-5-yl)-2, 1, 3-benzothiadiazole]-2′ , 2″-diyl) (F8TBT) with the time-of-flight (TOF) technique. These blends are used in efficient all-polymer photovoltaic devices. They found that the hole mobility in the neat P3HT is about two to three times larger than the hole mobility in the blend with F8TBT. Additionally, the blend exhibits a negative field dependence while the neat P3HT film displays a positive field dependence. These results are in qualitative agreement with the calculated field dependence reported here (see Fig. 2).

SCL diodes are a much used way of measuring the mobility in organic materials. In such a device the injection of one carrier species is reduced, by careful selection of the electrode materials, while the contacts can inject and extract more carriers than the bulk can carry. The resulting current density is proportional to the charge carrier mobility[43]

$$J_{\mathrm{SCL}}=\frac{9}{8}\varepsilon\mu\frac{V^2}{L^3} \tag{8}$$

for a constant mobility. This technique has been applied to neat and blend materials alike. For neat materials both en-

hancements can yield an increase in mobility. Experimentally, an enhancement [beyond the quadratic behavior described by Eq. (8)] of the current density at high applied voltages is often observed. In a SCL device increasing the applied voltage enhances both the electric field *and* the carrier density. It is therefore not *a priori* clear whether this enhancement stems from the field dependence, the density dependence of the mobility, or a combination of the two.

Empirically the mobility has been described by a stretched exponential,[44,45]

$$\mu = \mu_0 e^{\gamma\sqrt{F}}, \tag{9}$$

where $\gamma$ is the field activation parameter. Murgatroyd showed that the resulting SCL current is given by[46]

$$J_{\mathrm{SCL}} = \frac{9}{8}\varepsilon\mu_0\frac{V^2}{L^3}e^{0.891\gamma\sqrt{V/L}}, \tag{10}$$

where the electric field has been approximated by $F \approx V/L$. The parameter $\gamma$ reflects the lowering of hopping barriers in the direction of the electric field. A field dependent mobility of the form given by Eq. (9) was used to fit SCL currents in conjugated polymers and blends thereof.[47,48] This procedure makes possible the quantification of the apparent bias dependence of the mobility, but it ignores the density dependence of mobility and is, therefore, not strictly correct. In fact, Tanase *et al.* showed that the enhancement of the SCL hole current in diodes made of PPV derivatives originates from the density dependence of the mobility rather than from its field dependence, at least at room temperature.[37] In the present context, this equation is only used to make possible a comparison of the simulated mobility data (Figs. 1 and 2) with experimental results from the literature. It should be noted that for the correct interpretation of current-voltage data it might be necessary to correct for the series resistance of the substrates.[49] If this is done incorrectly, the extracted value of $\gamma$ will be incorrect.

The mobility data plotted in Fig. 2 bear out a positive field dependence for high carrier densities and a negative field dependence at low densities. So, for low densities the effects of increasing carrier density and electric field are opposite, while they both enhance the mobility at high carrier densities. In a SCL diode the carrier density is highest at the injecting contact, where the field is low, and relatively low in the bulk of the active layer, where the field is larger.[43] Hence, it is not immediately obvious whether the resulting bias voltage dependence is positive or negative. Experimentally, both types of behavior have been observed.[47]

To assess the voltage dependence of the SCL current in blends we have used the mobility data for a blend of average feature size $b=6$ nm and for neat material in a one-dimensional continuum model. The current density in this model is given by

$$J = qn(x)\mu(x)F(x) - kT\mu(x)\frac{dn(x)}{dx}, \tag{11}$$

where $n(x)$ and $F(x)$ are the local carrier density and field, respectively. This equation is solved self-consistently together with the Poisson equation $dF/dx=(q/\varepsilon)n(x)$. This procedure requires the mobility be known as a function of carrier density and electric field strength. The mobility at densities and fields other than those plotted in Figs. 1 and 2 are obtained by bilinear interpolation of those data. Briefly, the mobility is linearly interpolated in field and density directions to obtain the mobility at the desired density and field.[50] To gauge the accuracy of this interpolation procedure the resulting current-voltage characteristic for neat material was compared with that calculated using the parametrization of the mobility in neat material given by Pasveer *et al.*[25] Excellent agreement was found between the simulations (data not shown).

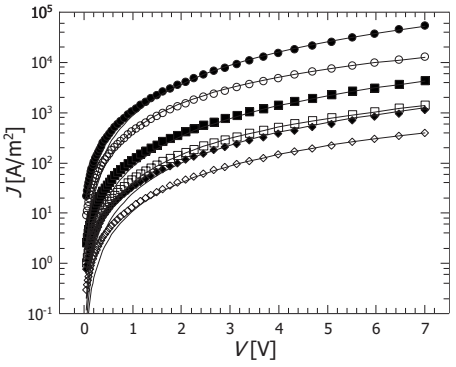


FIG. 6. Calculated space-charge-limited currents for a neat polymer (closed) and a 1:1 blend with average feature size $b=6$ nm (open) of different thicknesses (circles 100 nm, squares 200 nm, and diamonds 300 nm). The lines denote fits to Eq. (10).

Figure 6 displays the simulated current-voltage characteristics for neat and blend materials. The data are fitted to Eq. (10) and the extracted zero-field mobilities $\mu_0$ and field activation parameters $\gamma$ listed in Table I. For both materials, the extracted zero-field mobility has a slight dependence on thickness.[51] The zero-field mobilities for the blend material are approximately a factor of 2–3 lower than the ones obtained for the neat material. The field activation parameters $\gamma$ are quite different though: For the thicknesses studied the $\gamma$'s are negative. These results indicate that the experimentally observed negative $\gamma$ values[47] can be a result of blend morphology. However, we stress that this is by no means general: The complex balance between field and density dependences of the mobility ultimately determines $\gamma$ and this will depend on the exact blend morphology as well as on other material parameters.

Of course, the predicted results will not apply to all blend systems. In our model it is tacitly assumed that the blend's morphology does not influence the hopping rates $W_{i\to j}$

TABLE I. Zero-field mobilities $\mu_0$ and field-activation parameters $\gamma$ obtained by fitting the data in Fig. 6 to Eq. (10).

| $L$ | 100 nm | 200 nm | 300 nm |
|---|---|---|---|
| $\mu_0$(neat) [m$^2$/V s] | $2.6\times10^{-8}$ | $2.2\times10^{-8}$ | $2.2\times10^{-8}$ |
| $\gamma$(neat) [$\sqrt{m/V}$] | $4\times10^{-5}$ | $1\times10^{-5}$ | $1\times10^{-5}$ |
| $\mu_0$(blend) [m$^2$/V s] | $1.3\times10^{-8}$ | $9.3\times10^{-9}$ | $8.0\times10^{-9}$ |
| $\gamma$(blend) [$\sqrt{m/V}$] | $-9\times10^{-5}$ | $-9\times10^{-5}$ | $-9\times10^{-5}$ |

within the constituent phases. This may not always be true as the crystallinity or polymer chain orientation may well change by blending one material with another material. Indeed some studies demonstrate that the mobility in blends of an asymmetrically substituted poly(*p*-phenylene vinylene) (PPV) with [6,6]-phenyl-$C_{61}$-butyric acid methyl ester (PCBM) critically depends on the ratio of PPV to PCBM: The hole mobility in the PPV phase is found to be enhanced by more than two orders of magnitude as compared with its neat value when the PPV is blended with up to 80% (by weight) of PCBM.[52–54] Melzer *et al.*[52] suggested that this enhancement of the mobility might be caused by a frustration of the circular conformation adopted by the polymer chains in neat films of this PPV derivative.[55] On the other hand, it must be noted that this enhancement is not found for all PPVs or, indeed, conjugated polymers, stressing the need to take into account the morphology of the device when interpreting data taken by experiment.

## IV. SUMMARY AND CONCLUSIONS

In sum, charge transport in disordered organic blends has been studied theoretically by numerically solving the Pauli master equation. The influence of morphology, disorder, electric field, and charge carrier concentration on blend mobility are studied. Important differences between neat materials and blends are found: While for neat materials field and density dependences can be factorized, such a factorization is not possible for blends. Moreover, at low charge carrier densities blend mobility is found to decrease with increasing field, in agreement with recent TOF measurements on polymer blends.[42] As regards the impact of the volume ratio of the constituent materials and their domain-size charge transport is favored by relatively large domains, especially for strongly disordered materials.

In order to relate the predicted field and density dependences to mobility measurements in space-charge-limited diodes, the current density in such devices was simulated. It has been found that, for the parameters and morphologies studied, the apparent mobility in such a device decreases with increasing bias voltage. Experimentally this type of behavior was reported by Huang *et al.*[47] However, other researches did not find such a negative apparent field activation parameter $\gamma$ indicating that the importance of characterizing the blend morphology.

## ACKNOWLEDGMENTS

R. A. J. Janssen, C. Groves, and C. R. McNeill are gratefully acknowledged for many stimulating discussions. This work was supported by the Deutsche Forschungsgemeinschaft under Priority Program 1355 "Elementary Processes of Organic Photovoltaics."

[1] R. H. Friend, R. W. Gymer, A. B. Holmes, J. H. Burroughes, R. N. Marks, C. Taliani, D. D. C. Bradley, D. A. Dos Santos, J. L. Brédas, M. Löglund, and W. R. Salaneck, Nature (London) **397**, 121 (1999).
[2] A. Dodabalapur, Mater. Today **9**, 24 (2006).
[3] C. J. Brabec, N. S. Sariciftci, and J. C. Hummelen, Adv. Funct. Mater. **11**, 15 (2001).
[4] K. M. Coakley and M. D. McGehee, Chem. Mater. **16**, 4533 (2004).
[5] P. Peumans, S. Uchida, and S. R. Forrest, Nature (London) **425**, 158 (2003).
[6] C. R. McNeill and N. C. Greenham, Adv. Mater. **21**, 3840 (2009).
[7] G. Yu, A. J. Heeger, and R. D. Rieke, Synth. Met. **72**, 249 (1995).
[8] X. L. Chen and S. A. Jenekhe, Macromolecules **30**, 1728 (1997).
[9] M. Bronner, A. Opitz, and W. Brütting, Phys. Status Solidi A **205**, 549 (2008).
[10] A. Kumar, M. A. Baklar, K. Scott, T. Kreouzis, and N. Stingelin-Stutzmann, Adv. Mater. **21**, 4447 (2009).
[11] M. Berggren, O. Inganäs, G. Gustafsson, J. Rasmusson, M. R. Anersson, T. Hjertberg, and O. Wennerström, Nature (London) **372**, 444 (1994).
[12] P. Gomes da Costa and E. M. Conwell, Phys. Rev. B **48**, 1993 (1993).
[13] R. N. Marks, J. J. M. Halls, D. D. C. Bradley, R. H. Friend, and A. B. Holmes, J. Phys.: Condens. Matter **6**, 1379 (1994).
[14] S. Barth and H. Bässler, Phys. Rev. Lett. **79**, 4445 (1997).
[15] J. M. Frost, F. Cheynis, S. M. Tuladhar, and J. Nelson, Nano Lett. **6**, 1674 (2006).
[16] L. Meng, Y. Shang, Q. Li, Y. Li, X. Zhan, Z. Shuai, R. G. E. Kimber, and A. B. Walker, J. Phys. Chem. B **114**, 36 (2010).
[17] H. Hoppe, T. Glatzel, M. Niggemann, W. Schwinger, F. Schaeffler, A. Hinsch, M. Ch. Lux-Steiner, and N. S. Sariciftci, Thin Solid Films **511-512**, 587 (2006).
[18] C. R. McNeill, J. J. M. Halls, R. Wilson, G. L. Whiting, S. Berkebile, M. G. Ramsey, R. H. Friend, and N. C. Greenham, Adv. Funct. Mater. **18**, 2309 (2008).
[19] J.-S. Kim, P. K. H. Ho, C. E. Murphy, and R. H. Friend, Macromolecules **37**, 2861 (2004).
[20] D. C. Coffey, O. G. Reid, D. B. Rodovsky, G. P. Bartholomew, and D. S. Ginger, Nano Lett. **7**, 738 (2007).
[21] C. M. Björström, A. Bernasik, J. Rysz, A. Budkowski, S. Nilsson, M. Svensson, M. R. Andersson, K. O. Magnusson, and E. Moons, J. Phys.: Condens. Matter **17**, L529 (2005).
[22] A. C. Arias, F. Endicott, and R. A. Street, Adv. Mater. **18**, 2900 (2006).
[23] C. Groves, L. J. A. Koster, and N. C. Greenham, J. Appl. Phys. **105**, 094510 (2009).
[24] Z. G. Yu, D. L. Smith, A. Saxena, R. L. Martin, and A. R. Bishop, Phys. Rev. B **63**, 085202 (2001).
[25] W. F. Pasveer, J. Cottaar, C. Tanase, R. Coehoorn, P. A. Bobbert, P. W. M. Blom, D. M. de Leeuw, and M. A. J. Michels, Phys. Rev. Lett. **94**, 206601 (2005).
[26] E. Tutiš, I. Batistić, and D. Berner, Phys. Rev. B **70**, 161202(R) (2004).

[27] J. J. M. van der Holst, M. A. Uijttewaal, B. Ramachandhran, R. Coehoorn, P. A. Bobbert, G. A. de Wijs, and R. A. de Groot, Phys. Rev. B **79**, 085203 (2009).
[28] J. Zhou, Y. C. Zhou, J. M. Zhao, C. Q. Wu, X. M. Ding, and X. Y. Hou, Phys. Rev. B **75**, 153201 (2007).
[29] P. K. Watkins, A. B. Walker, and G. L. B. Verschoor, Nano Lett. **5**, 1814 (2005).
[30] S. Heun and P. M. Borsenberger, Chem. Phys. **200**, 245 (1995).
[31] J. Rommens, M. Van der Auweraer, F. C. De Schryver, D. Terrell, and S. De Meutter, J. Phys. Chem. **100**, 10673 (1996).
[32] H. C. F. Martens, P. W. M. Blom, and H. F. M. Schoo, Phys. Rev. B **61**, 7489 (2000).
[33] Y. Shen, K. Diest, M. H. Wong, B. R. Hsieh, D. H. Dunlap, and G. G. Malliaras, Phys. Rev. B **68**, 081204(R) (2003).
[34] O. Tal, Y. Rosenwaks, Y. Preezant, N. Tessler, C. K. Chan, and A. Kahn, Phys. Rev. Lett. **95**, 256405 (2005).
[35] R. Coehoorn, W. F. Pasveer, P. A. Bobbert, and M. A. J. Michels, Phys. Rev. B **72**, 155206 (2005).
[36] C. Tanase, E. J. Meijer, P. W. M. Blom, and D. M. de Leeuw, Phys. Rev. Lett. **91**, 216601 (2003).
[37] C. Tanase, P. W. M. Blom, and D. M. de Leeuw, Phys. Rev. B **70**, 193202 (2004).
[38] C. Tanase, P. W. M. Blom, D. M. de Leeuw, and E. J. Meijer, Phys. Status Solidi A **201**, 1236 (2004).
[39] H. Bässler, Phys. Status Solidi B **175**, 15 (1993).
[40] J. Stephan, A. Liemant, F. Albrecht, and L. Brehmer, Synth. Met. **109**, 327 (2000).
[41] K. D. Meisel, W. F. Pasveer, J. Cottaar, C. Tanase, R. Coehoorn P. A. Bobbert, P. W. M. Blom, D. M. de Leeuw, and M. A. J. Michels, Phys. Status Solidi C **3**, 267 (2006).
[42] C. R. McNeill and N. C. Greenham, Appl. Phys. Lett. **93**, 203310 (2008).
[43] M. A. Lampert and P. Mark, *Current Injection in Solids* (Academic Press, New York, 1970).
[44] D. M. Pai, J. Chem. Phys. **52**, 2285 (1970); W. D. Gill, J. Appl. Phys. **43**, 5033 (1972); L. B. Schein, A. Peled, and D. Glatz, *ibid.* **66**, 686 (1989); P. M. Borsenberger, *ibid.* **68**, 6263 (1990); M. A. Abkowitz, Philos. Mag. B **65**, 817 (1992).
[45] P. W. M. Blom, M. J. M. de Jong, and M. G. van Munster, Phys. Rev. B **55**, R656 (1997); M. C. J. M. Vissenberg and P. W. M. Blom, Synth. Met. **102**, 1053 (1999); H. C. F. Martens, H. B. Brom, and P. W. M. Blom, Phys. Rev. B **60**, R8489 (1999).
[46] P. N. Murgatroyd, J. Phys. D **3**, 151 (1970).
[47] F. Huang, K.-S. Chen, H.-L. Yip, S. K. Hau, O. Acton, Y. Zhang, J. Luo, and A. K.-Y. Jen, J. Am. Chem. Soc. **131**, 13886 (2009).
[48] A. Gadisa, X. Wang, S. Admassie, E. Perzon, F. Oswald, F. Langa, M. R. Andersson, and O. Inganäs, Org. Electron. **7**, 195 (2006).
[49] V. D. Mihailetchi, J. K. J. van Duren, P. W. M. Blom, J. C. Hummelen, R. A. J. Janssen, J. M. Kroon, M. T. Rispens, W. J. H. Verhees, and M. M. Wienk, Adv. Funct. Mater. **13**, 43 (2003).
[50] W. H. Press, B. P. Flannery, S. A. Teukolsky, and W. T. Vetterling, *Numerical Recipes in Pascal*, 1st ed. (Cambridge University Press, Cambridge, 1989), p. 108.
[51] S. L. M. van Mensfoort and R. Coehoorn, Phys. Rev. B **78**, 085207 (2008).
[52] C. Melzer, E. Koop, V. D. Mihailetchi, and P. W. M. Blom, Adv. Funct. Mater. **14**, 865 (2004).
[53] V. D. Mihailetchi, L. J. A. Koster, P. W. M. Blom, C. Melzer, B. de Boer, J. K. J. van Duren, and R. A. J. Janssen, Adv. Funct. Mater. **15**, 795 (2005).
[54] S. M. Tuladhar, D. Poplavskyy, S. A. Choulis, J. R. Durrant, D. D. C. Bradley, and J. Nelson, Adv. Funct. Mater. **15**, 1171 (2005).
[55] M. Kemerink, J. K. J. van Duren, P. Jonkheijm, W. F. Pasveer, P. M. Koenraad, R. A. J. Janssen, H. W. M. Salemink, and J. H. Wolter, Nano Lett. **3**, 1191 (2003).